Article

[DRAFT] On the Single-Sideband Transform for MVDR Beamformers

Vitor Curtarelli [1,*], Israel Cohen [1]

1 Andrew and Erna Viterbi Faculty of Electrical and Computer Engineering, Technion–Israel Institute of Technology, Technion City, Haifa 3200003, Israel

* Correspondence: vitor.c@campus.technion.ac.il

Abstract: This paper investigates the application of the Single-Sideband Transform (SSBT) for constructing a Minimum-Variance Distortionless-Response (MVDR) beamformer in the context of the convolutive transfer function (CTF) model for short-windows time-frequency transforms. Our study aims to optimize the utilization of SSBT in this endeavor, by examining its characteristics and traits. We address a reverberant scenario with multiple noise sources, aiming to minimize both undesired interference and reverberation in the output. Through simulations reflecting real-life scenarios, we show that employing the SSBT, both in a naive and a refined approach, results in superior signal enhancement compared to the Short-Time Fourier Transform (STFT). The refined approach not only enhances the signal but also ensures the desired distortionless behavior, which is not achieved by the naive one.

Keywords: Single-sideband transform; MVDR beamformer; Filter banks; Array signal processing; Signal enhancement.

1. Introduction

Beamformers are an important tool for signal enhancement, having a plethora of applications from hearing aids [1] to source localization [2] to imaging [3,4]. Traditionally, beamforming techniques are used either strictly on the time domain, strictly on the frequency domain, or on the time-frequency domain [5], the later allowing the exploitation of frequency-related information while also dynamically adapting to signal changes over time. While the Short-Time Fourier Transform (STFT) is widely used for time-frequency analysis [6,7], alternative transforms [8–10] can also be employed, offering unique perspectives on signal analysis.

Among these, the Single-Sideband Transform (SSBT) [11,12], stands out for its real-valued frequency spectrum. It has been shown that the SSBT works particularly well with short analysis windows [11], lending itself useful when working with the convolutive transfer function (CTF) model [13] and filter-banks [14,15] for signal analysis.

Two of the most important goals in beamforming are output noise minimization and the distortionless-ness of the desired signal, both being achieved by the Minimum-Variance Distortionless-Response (MVDR) beamformer [16,17]. As the MVDR beamformer works

Citation: Curtarelli, V.; Cohen, I. On the Single-Sideband Transform for MVDR Beamformers. *Algorithms* **2023**, *1*, 0. https://doi.org/

Received:
Revised:
Accepted:
Published:

on the frequency (or time-frequency) domain without any specification on the transform chosen, it is of interest to explore and compare the performance of this filter, when designing it through different time-frequency transforms.

Motivated by this, our paper explores the SSB transform and its application on the subject of beamforming within the context of the CTF model. We propose an approach for the CTF that allows the separation of desired and undesired speech components for reverberant environments, and employ this approach for designing the MVDR beamformer. We also explore the limitations and traits of the SSBT, and how to properly adapt the MVDR beamformer to this new transform's constraints.

We organized the paper as follows: in Section 2 we introduce the proposed time-frequency transforms, how they're related and which qualities from each are relevant; Section 3 the signal model considered in the time domain is presented, and how it is transferred into the time-frequency domain within the considered framework; and in Section 4 we develop a true-MVDR beamformer with the SSBT, taking into account its features. In Section 5 we present and discuss the results, comparing the studied methods and beamforming techniques obtained. Finally, in Section 6 we conclude this paper.

2. STFT and Single-Sideband Transform

When studying signals and systems, often frequency and time-frequency transforms are used in order to change the signal domain [18], allowing the exploitation of different patterns and informations that are inherent to the signal.

Given a time-domain signal $x[n]$, its Short-time Fourier Transform (STFT) [6,7] is given by

$$X_{\mathcal{F}}[l,k] = \sum_{n=0}^{K-1} w[n]x[n - l \cdot O]e^{-\mathrm{j}2\pi k \frac{(n-l \cdot O)}{K}} \tag{1}$$

where $w[n]$ is an analysis window of length K; and O is the overlap between windows of the transform, usually $O = \lfloor K/2 \rfloor$. Even though the STFT is the most traditionally used time-frequency transform, it isn't the only one available. Thus, exploring different possibilities for such an operation can be useful and lead to interesting results.

The Single-Sideband Transform (SSBT) [11] is one such alternative, in which the frequency values are cleverly calculated such that its spectrum is real-valued, without loss of information. The SSB transform of $x[n]$ is defined as

$$X_{\mathcal{S}}[l,k] = \sqrt{2}\Re\left\{ \sum_{n=0}^{L-1} w[n]x[n - l \cdot O]e^{\mathrm{j}2\pi k \frac{(n-l \cdot O)}{K} + \mathrm{j}\frac{3\pi}{4}} \right\} \tag{2}$$

Assuming that $x[n]$ is real-valued, one advantage of using the STFT is that we only need to work with $\left\lfloor \frac{K+1}{2} \right\rfloor + 1$ frequency bins, given its complex-conjugate behavior. Meanwhile, the SSBT needs to use all K possible bins to correctly capture all information of $x[n]$, however it is real-valued.

From Eq. (2) it's easy to see that

$$\begin{aligned} X_{\mathcal{S}}[l,k] &= \sqrt{2}\Re\left\{ X_{\mathcal{F}}[l,k]e^{\mathrm{j}\frac{3\pi}{4}} \right\} \\ &= -\Re\{X_{\mathcal{F}}[l,k]\} + \Im\{X_{\mathcal{F}}[l,k]\} \end{aligned} \tag{3}$$

assuming that all K bins of the STFT are available.

One disadvantage with the SSBT is that the convolution theorem does not hold when employing it (see Appendix A), not even as an approximation. Nonetheless, by first converting any result in the SSBT domain to the STFT domain (using Eq. (3)) before utilization, it remains feasible to employ the obtained values for estimating matrices and signals.

3. Signal and Array Model

Let there be a generic sensor array, comprised of M sensors, within a reverberant environment. In this setting there also are a desired and an interfering sources (namely $x[n]$ and $v[n]$), and also uncorrelated noise $r_m[n]$ (at each sensor m), all travelling with a speed c. We assume that the sources are spatially stationary, and all discrete signals were sampled with the same sampling frequency f_s.

We denote $h_m[n]$ as the room impulse response between the desired source and the m-th sensor. We similarly define $g_m[n]$ for the interfering source. From this, we write $y_m[n]$ as the observed signal at the m-th sensor as

$$y_m[n] = h_m[n] * x[n] + g_m[n] * v[n] + r_m[n] \tag{4}$$

We let m' be the reference sensor's index, for simplicity assume $m' = 1$. We let $x_1[n] = h_1[n] * x[n]$ (and similarly for $v_1[n]$). $b_m[n]$ is the *relative* impulse response between the desired signal (at the reference sensor) and the m-th sensor, define such that

$$b_m[n] * x_1[n] = h_m[n] * x[n] \tag{5}$$

We similarly define $c_m[n]$ such that $c_m[n] * v_1[n] = g_m[n] * v[n]$. Therefore, Eq. (4) becomes

$$y_m[n] = b_m[n] * x_1[n] + c_m[n] * v_1[n] + r_m[n] \tag{6}$$

We can use a time-frequency transform (here the STFT or the SSBT[1], exposed in Section 2) with the CTF model [13] to turn Eq. (6) into

$$Y_m[l,k] = B_m[l,k] * X_1[l,k] + C_m[l,k] * V_1[l,k] + R_m[l,k] \tag{7}$$

where $Y_m[l,k]$ is the transform of $y_m[n]$ (resp. all other signals); l is the window index, and k the bin index, with $0 \leq k \leq K-1$; and the convolution is in the window-index axis.

Using that $B_m[l,k]$ is a finite (possibly truncated) response with L_B windows, then

$$B_m[l,k] * X_1[l,k] = \mathbf{b}_m^{\mathsf{T}}[k]\mathbf{x}_1[l,k] \tag{8}$$

in which

$$\mathbf{b}_m[k] = \Big[\ B_m[-\Delta,k]\,,\ \cdots,\ B_m[0,k]\,,\ \cdots,\ B_m[L_B-\Delta-1,k]\ \Big]^{\mathsf{T}} \tag{9a}$$

$$\mathbf{x}_1[l,k] = \Big[\ X_1[l+\Delta,k]\,,\ \cdots,\ X_1[l,k]\,,\ \cdots,\ X_1[l-L_B+\Delta+1,k]\ \Big]^{\mathsf{T}} \tag{9b}$$

and in the same way we define $\mathbf{c}_m[k]$ and $\mathbf{v}_1[l,k]$; where $\mathbf{b}_m[k]$, $x_1[l,k]$, $\mathbf{c}_m[k]$ and $v_1[l,k]$ are non-causal, given that they are relative to the first sensor.

[1] Although the SSBT doesn't hold the convolution theorem, we will assume it does for the purpose of the formulation.

Note that $\mathbf{b}_m[k]$ doesn't depend on the index l, since neither the environment nor the source's position change over time. With this, Eq. (7) becomes

$$Y_m[l,k] = \mathbf{b}_m^{\mathsf{T}}[k]\mathbf{x}_1[l,k] + \mathbf{c}_m^{\mathsf{T}}[k]\mathbf{v}_1[l,k] + R_m[l,k] \tag{10}$$

Vectorizing the signals sensor-wise, we finally get

$$\mathbf{y}[l,k] = \mathbf{B}^{\mathsf{T}}[k]\mathbf{x}_1[l,k] + \mathbf{C}^{\mathsf{T}}[k]\mathbf{v}_1[l,k] + \mathbf{r}[l,k] \tag{11}$$

where

$$\mathbf{y}[l,k] = \left[\, y_1[l,k]\,,\ \cdots\,,\ y_M[l,k]\,\right]^{\mathsf{T}} \tag{12}$$

and similarly for the other variables. In this situation, $\mathbf{B}[k]$ and $\mathbf{C}[k]$ are $L_B \times M$ and $L_C \times M$ matrices respectively; $\mathbf{x}_1[l,k]$ and $\mathbf{v}_1[l,k]$ are $L_B \times 1$ and $L_C \times 1$ vectors respectively; and $\mathbf{y}[l,k]$ and $\mathbf{r}[l,k]$ are $M \times 1$ vectors.

3.1. Reverb-aware formulation

We let the 0-th window of $\mathbf{B}[k]$ be the desired-speech frequency response (named $\mathbf{d}_x[k]$), with the rest being (both forward and backwards in time) an undesired component, comprised only of reverberation.

With this, we write

$$\mathbf{B}^{\mathsf{T}}[k]\mathbf{x}_1[l,k] = \mathbf{d}_x[k]X_1[l,k] + \sum_{\substack{l'=-\Delta \\ l'\neq 0}}^{L_B-\Delta-1} \mathbf{p}_{B,l'}[k]X_1[l-l',k] \tag{13}$$

where $\mathbf{p}_{B,l'}[k]$ is the l'-th row of $\mathbf{B}[k]$. With this, $\mathbf{d}_x[k]X_1[l,k]$ is the desired speech component of $\mathbf{B}^{\mathsf{T}}[k]\mathbf{x}_1[l,k]$, and the summation over l' is the undesired component. We will call $\mathbf{d}_x[k]$ the desired-speech frequency response.

We define $\mathbf{q}_{C,l''}$ similarly, such that

$$\mathbf{C}^{\mathsf{T}}[k]\mathbf{v}_1[l,k] = \sum_{l''=-\Delta}^{L_C-\Delta-1} \mathbf{q}_{C,l''}[k]V_1[l-l'',k] \tag{14}$$

From here, we can write

$$\mathbf{y}[l,k] = \mathbf{d}_x[k]X_1[l,k] + \mathbf{w}[l,k] \tag{15}$$

with $\mathbf{w}[l,k]$ being the undesired signal (undesired speech components + interfering source + noise), given by

$$\mathbf{w}[l,k] = \sum_{\substack{l'=-\Delta \\ l'\neq 0}}^{L_B-\Delta-1} \mathbf{p}_{B,l'}[k]X_1[l-l',k] + \sum_{l''=-\Delta}^{L_C-\Delta-1} \mathbf{q}_{C,l''}[k]V_1[l-l'',k] + \mathbf{r}[l,k] \tag{16}$$

Note that in Eqs. (15) and (16) we can treat each window of the incoming signals as a different source, with its own frequency response, which allows the use of traditional methods for signal enhancement.

It's important to have in mind the sensor delay and window length. If the time for the signal to travel from the reference to the farthest sensor exceeds the window length (in seconds), multiple windows may represent the desired speech. This isn't a problem if $\frac{\delta}{c} < \frac{K}{f_s}$, where δ is the distance to the farthest sensor, and K is the window length.

for simplicity we assume that $X_1[l_1, k]$ is independent of $X_1[l_2, k]$, and each component of $\mathbf{w}[l, k]$ is independent of the other, and of $\mathbf{d}_x[k]X_1[l - \Delta, k]$. This isn't strictly true, given both the time-frequency windowing process and the reverberant behavior of the environment.

3.2. MVDR beamformer

We use a linear time-variant filter $\mathbf{f}[l, k]$ to estimate the desired signal at the reference sensor, such that

$$\begin{aligned} Z[l, k] &= \mathbf{f}^{\mathsf{H}}[l, k]\mathbf{y}[l, k] \\ &\approx X_1[l, k] \end{aligned} \tag{17}$$

with $(\cdot)^{\mathsf{H}}$ being the transposed-complex-conjugate operator. This filter is time-invariant within each window, but it may change over time to adapt to the signals.

In order to minimize $\mathbf{w}[l, k]$ the MVDR beamformer [17] will be used, being given by

$$\mathbf{f}^{\star}[l, k] = \min_{\mathbf{f}[l,k]} \mathbf{f}[l, k]^{\mathsf{H}}\mathbf{\Phi}_{\mathbf{w}}[l, k]\mathbf{f}[l, k] \text{ s.t. } \mathbf{f}^{\mathsf{H}}[l, k]\mathbf{d}_x[k] = 1 \tag{18}$$

in which $\mathbf{f}^{\mathsf{H}}[l, k]\mathbf{d}_x[k] = 1$ is the distortionless constraint, and $\mathbf{\Phi}_{\mathbf{w}}[l, k]$ is the correlation matrix of the undesired signal,

$$\begin{aligned} \mathbf{\Phi}_{\mathbf{w}}[l, k] = &\sum_{\substack{l'=-\Delta \\ l'\neq 0}}^{L_B-\Delta-1} \mathbf{p}_{B,l'}^{\mathsf{H}}[k]\mathbf{p}_{B,l'}[k]\phi_{X_1}[l - l', k] \\ &+ \sum_{l''=-\Delta}^{L_C-\Delta-1} \mathbf{q}_{C,l''}^{\mathsf{H}}[k]\mathbf{q}_{C,l''}[k]\phi_{V_1}[l - l'', k] \\ &+ \mathbf{I}_M\phi_R[l, k] \end{aligned} \tag{19}$$

where $\phi_{X_1}[l, k]$ is the variance of $X_1[l, k]$ (same for $\phi_{V_1}[l, k]$ and $\phi_R[l, k]$), and $\mathbf{I}_M$ is the $M \times M$ identity matrix, under the premise that the distribution of $\mathbf{r}[l, k]$ is the same for all sensors.

The solution to Eq. (18) is

$$\mathbf{f}_{\text{mvdr}}[l, k] = \frac{\mathbf{\Phi}_{\mathbf{w}}^{-1}[l, k]\mathbf{d}_x[k]}{\mathbf{d}_x^{\mathsf{H}}[k]\mathbf{\Phi}_{\mathbf{w}}^{-1}[l, k]\mathbf{d}_x[k]} \tag{20}$$

3.3. Beamformer metrics

Considering the problem, the relevant metrics are the narrowband- gain in signal-to-noise ratio (SNR) and desired signal distortion index (DSDI), respectively given by

$$\text{gSNR}[l, k] = \phi_{V_1}[l, k]\frac{\left|\mathbf{f}^{\mathsf{H}}[l, k]\mathbf{d}_x[k]\right|^2}{\mathbf{f}^{\mathsf{H}}[l, k]\mathbf{\Phi}_{\mathbf{w}}[l, k]\mathbf{f}[l, k]} \tag{21}$$

$$v[l, k] = \left|\mathbf{f}^{\mathsf{H}}[l, k]\mathbf{d}_x[k] - 1\right|^2 \tag{22}$$

We can also define the window-averaged gSNR and DSDI as

$$\mathrm{gSNR}[k] = \frac{1}{L_Z}\sum_{l=0}^{L_Z-1} \mathrm{gSNR}[l,k] \tag{23}$$

$$v[k] = \frac{1}{L_Z}\sum_{l=0}^{L_Z-1} v[l,k] \tag{24}$$

with L_Z being the number of windows of $Z[l,k]$.

4. True-MVDR with the SSB Transform

When using the previous formulation with the SSBT, the distortionless constraint (in Eq. (18)) ensures that the beamformer avoids causing distortion exclusively within the SSBT domain. However, as explained towards the end of Section 2, the SSBT beamformer must undergo conversion into the STFT domain (via Eq. (3)) before filtering due to the transform's limitations. To construct an SSBT beamformer that correctly adheres to the distortionless constraint, it is essential to consider this conversion step.

Given the signal $x[n]$, its STFT $X_{\mathcal{F}}[l,k]$ (with $\left\lfloor \frac{K+1}{2} + 1 \right\rfloor$ bins), and its SSBT $X_{\mathcal{S}}[l,k]$ (with K bins), from Eq. (3) it is possible to show[2] that

$$X_{\mathcal{F}}[l,k] = \frac{1}{\sqrt{2}}\left(e^{\mathrm{j}\frac{3\pi}{4}} X_{\mathcal{S}}[l,k] + e^{-\mathrm{j}\frac{3\pi}{4}} X_{\mathcal{S}}[l,K-k]\right) \tag{25}$$

From this, we propose a framework for the SSBT beamformer in which we consider both bins k and $K-k$ simultaneously. We define $\mathbf{w}'[l,k]$ as

$$\mathbf{w}'[l,k] = \begin{bmatrix} \mathbf{w}[l,k] \\ \mathbf{w}[l,K-k] \end{bmatrix}_{2M\times 1} \tag{26}$$

from which we define $\mathbf{\Phi}_{\mathbf{w}'}[l,k]$ as its correlation matrix. Under this idea, our filter $\mathbf{f}'[l,k]$ is a $2M \times 1$ vector, with the first M values being for the k-th bin, and the last M values for the $[K-k]$-th bin. With Eq. (25) it is easy to see that

$$\hat{\mathbf{f}}_{\mathcal{F}}[l,k] = \hat{\mathbf{A}}\mathbf{f}'[l,k] \tag{27}$$

where $\hat{\mathbf{A}}$ is

$$\hat{\mathbf{A}} = \begin{bmatrix} \frac{e^{\mathrm{j}\frac{3\pi}{4}}}{\sqrt{2}} & 0 & \cdots & 0 & \frac{e^{-\mathrm{j}\frac{3\pi}{4}}}{\sqrt{2}} & 0 & \cdots & 0 \\ 0 & \frac{e^{\mathrm{j}\frac{3\pi}{4}}}{\sqrt{2}} & \cdots & 0 & 0 & \frac{e^{-\mathrm{j}\frac{3\pi}{4}}}{\sqrt{2}} & \cdots & 0 \\ \vdots & \vdots & \ddots & \vdots & \vdots & \ddots & \vdots & \\ 0 & 0 & \cdots & \frac{e^{\mathrm{j}\frac{3\pi}{4}}}{\sqrt{2}} & 0 & 0 & \cdots & \frac{e^{-\mathrm{j}\frac{3\pi}{4}}}{\sqrt{2}} \end{bmatrix}_{M\times 2M} \tag{28}$$

and $\hat{\mathbf{f}}_{\mathcal{F}}[l,k]$ is the STFT-equivalent beamformer for $\mathbf{f}[l,k]$. From this, it is easy to see that the distortionless constraint for the STFT, within the SSBT domain, is

$$\mathbf{f}'^{\mathsf{H}}[l,k]\mathbf{D}_x[k] = 1 \tag{29}$$

[2] Eq. (25) (and its derivations) is invalid for $k=0$, and $k = K/2$ if K is even. In these cases $X_{\mathcal{F}}[l,k] = X_{\mathcal{S}}[l,k]$, and the "naive" SSBT beamformer from Section 3 works.

where $\mathbf{d}_{\mathcal{F};x}[l,k]$ is the desired-speech frequency response in the STFT domain; and

$$\mathbf{D}_x[k] = \hat{\mathbf{A}}^{\mathsf{H}}\mathbf{d}_{\mathcal{F};x}[k] \tag{30}$$

In this scheme, our minimization problem becomes

$$\mathbf{f}'^{\star}[l,k] = \min_{\mathbf{f}'[l,k]} \mathbf{f}'^{\mathsf{H}}[l,k]\mathbf{\Phi}_{\mathbf{w}'}[l,k]\mathbf{f}'[l,k] \text{ s.t. } \mathbf{f}'^{\mathsf{H}}[l,k]\mathbf{D}_x[k] = 1 \tag{31}$$

4.1. Real-valued SSBT true-MVDR beamformer

Although $\mathbf{\Phi}_{\mathbf{w}'}[l,k]$ is a matrix with real entries, $\mathbf{D}_x$'s entries are complex, and thus is the solution to Eq. (31), contradicting the purpose of utilizing the SSBT. To preserve this desired behavior, an additional constraint is necessary. Forcing $\mathbf{f}'[l,k]$ to be real (which will turn all $(\cdot)^{\mathsf{H}}$ into $(\cdot)^{\mathsf{T}}$, pure transpose), from the distortionless constraint of Eq. (29) we trivially have that

$$\mathbf{f}'^{\mathsf{T}}[l,k]\Re\{\mathbf{D}_x[k]\} = 1 \tag{32a}$$
$$\mathbf{f}'^{\mathsf{T}}[l,k]\Im\{\mathbf{D}_x[k]\} = 0 \tag{32b}$$

which can be put in matricial form,

$$\mathbf{f}'^{\mathsf{T}}[l,k]\mathbf{Q}_x[k] = \mathbf{i}^{\mathsf{T}} \tag{33}$$

with

$$\mathbf{Q}_x[k] = \Big[\, \Re\{\mathbf{D}_x[k]\}\,,\ \Im\{\mathbf{D}_x[k]\}\,\Big]_{2M\times 2} \tag{34a}$$
$$\mathbf{i} = \begin{bmatrix} 1 \\ 0 \end{bmatrix} \tag{34b}$$

With these manipulations, the minimization problem becomes

$$\mathbf{f}'^{\star}[l,k] = \min_{\mathbf{f}'[l,k]} \mathbf{f}'^{\mathsf{T}}[l,k]\mathbf{\Phi}_{\mathbf{w}'}[l,k]\mathbf{f}'[l,k] \text{ s.t. } \mathbf{f}'^{\mathsf{T}}[l,k]\mathbf{Q}_x[k] = \mathbf{i}^{\mathsf{T}} \tag{35}$$

whose formulation is the same as the linearly-constrained minimum variance (LCMV) [19] beamformer, and therefore its solution is

$$\mathbf{f}'^{\star}_{\text{mvdr}}[l,k] = \mathbf{\Phi}^{-1}_{\mathbf{w}'}[l,k]\mathbf{Q}_x[k]\left(\mathbf{Q}_x^{\mathsf{T}}[k]\mathbf{\Phi}^{-1}_{\mathbf{w}'}[k]\mathbf{Q}_x[k]\right)^{-1}\mathbf{i} \tag{36}$$

Using Eq. (27), we can obtain the desired beamformer $\hat{\mathbf{f}}^{\star}_{\mathcal{F}}[l,k]$, in the STFT domain.

5. Simulations

In the simulations[3], we employ a sampling frequency of 16kHz. The sensor array consists of a uniform linear array with 10 sensors spaced at 2cm. Room impulse responses were generated using Habets' RIR generator [20], and signals were selected from the SMARD [21] and LINSE [22] databases.

The room's dimensions are 4m × 6m × 3m (width × length × height), with a reverberation time of 0.11s. The desired source is located at (2m, 1m, 1m), it being a male voice

[3] Code is available at https://github.com/VCurtarelli/py-ssb-ctf-bf.

(SMARD, `50_male_speech_english_ch8_OmniPower4296.flac`). The interfering source, simulating an open door, is located simultaneously at $(0.5\text{m}, 5\text{m}, [0.3:0.3:2.7]\text{m})$, with a babble sound signal (LINSE database, `babble.mat`). The noise signal is white Gaussian noise (SMARD database, `wgn_48kHz_ch8_OmniPower4296.flac`). All signals were resampled to the desired frequency.

The sensor array is positioned at $(2\text{m}, [4.02:0.02:4.2]\text{m}, 1\text{m})$, with omnidirectional sensors of flat frequency response. The input SNR between desired and interfering signals is 5dB, and between desired and noise signals is 30dB. Filters are calculated every 25 windows, considering the previous 25 windows to calculate correlation matrices.

We compare filters obtained through the STFT and SSBT transforms. N-SSBT uses Eq. (20) to (naively) calculate the SSBT beamformer, and T-SSBT will denote the beamformer obtained via the true-distortionless MVDR from Section 4. Performance analysis is conducted via the STFT domain, with the SSBT beamformers being converted into it. In line plots, STFT is presented in red, N-SSBT in green, and T-SSBT in blue.

5.1. Results

In this scenario, we assume that the analysis windows have 32 samples. Fig. 1 shows the gain in SNR for each window (with the windows being represented by the time started, in seconds), and Fig. 2 the window-wise averaged gain in SNR, for all methods. In Fig. 3 we have the DSDI for all three methods, window-averaged.

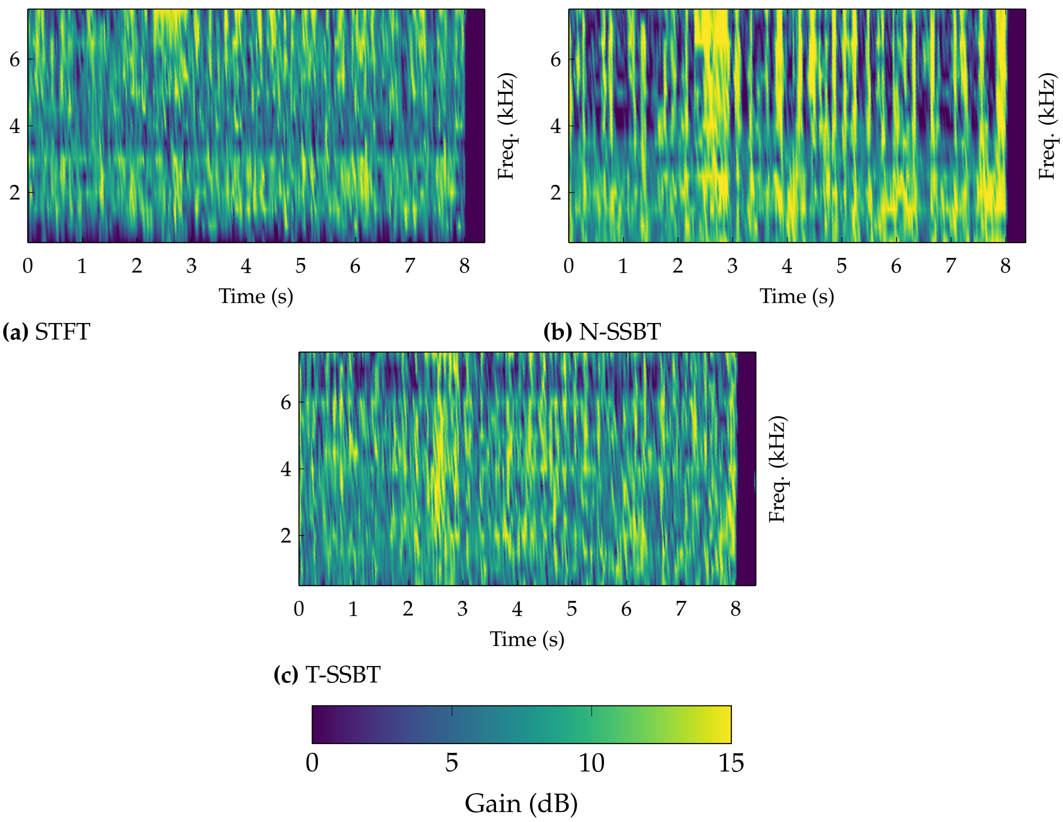

(a) STFT **(b)** N-SSBT **(c)** T-SSBT

Figure 1. Per-window SNR gain for 32 samples/window.

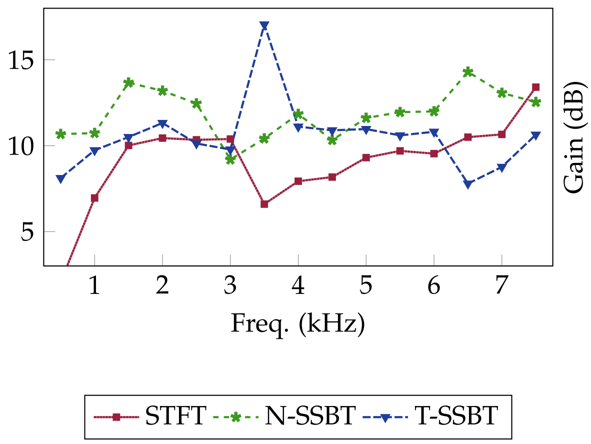

Figure 2. Window-average SNR gain for 32 samples/window.

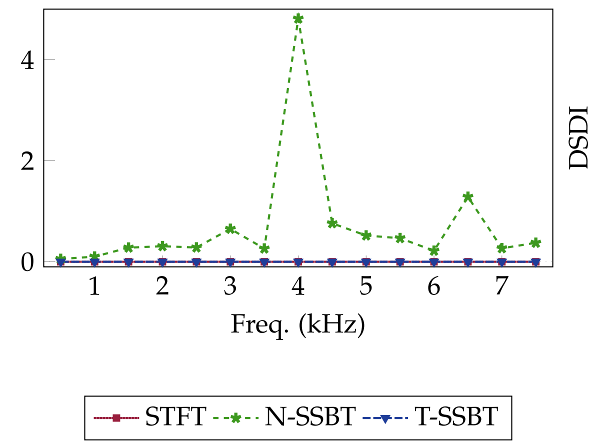

Figure 3. Window-average DSDI for 32 samples/window.

Although it isn't as clear from the per-window results of Fig. 1, Fig. 2 clearly shows that both SSBT beamformers had a better (at most equal) performance than the STFT one, with the N-SSBT beamformer having a better performance over (almost) all spectrum, and the T-SSBT beamformer being better for lower frequencies, tying with the STFT for higher ones.

Also, Fig. 3 shows that the T-SSBT filter was able to ensure a distortionless response for the desired signal, a feature that wasn't achieved by the N-SSBT beamformer. This was wholly expected, since the later was naively designed with the MVDR in mind, and wasn't fully planned to achieve a distortionless behavior in the STFT (and therefore the time) domain, while the T-SSBT took this into account on its derivation.

5.2. Results - 64 samples/window

In this simulation, we changed the number of samples per window from 32 to 64, keeping everything else the same.

In here, from Figs. 4 and 5 we see a similar result to that which was obtained previously, with the N-SSBT beamformer having a better performance overall but causing some distortion in the desired signal; and the T-SSBT beamformer having a slightly better performance STFT one while also having a distortionless behavior, as is seen in Fig. 6.

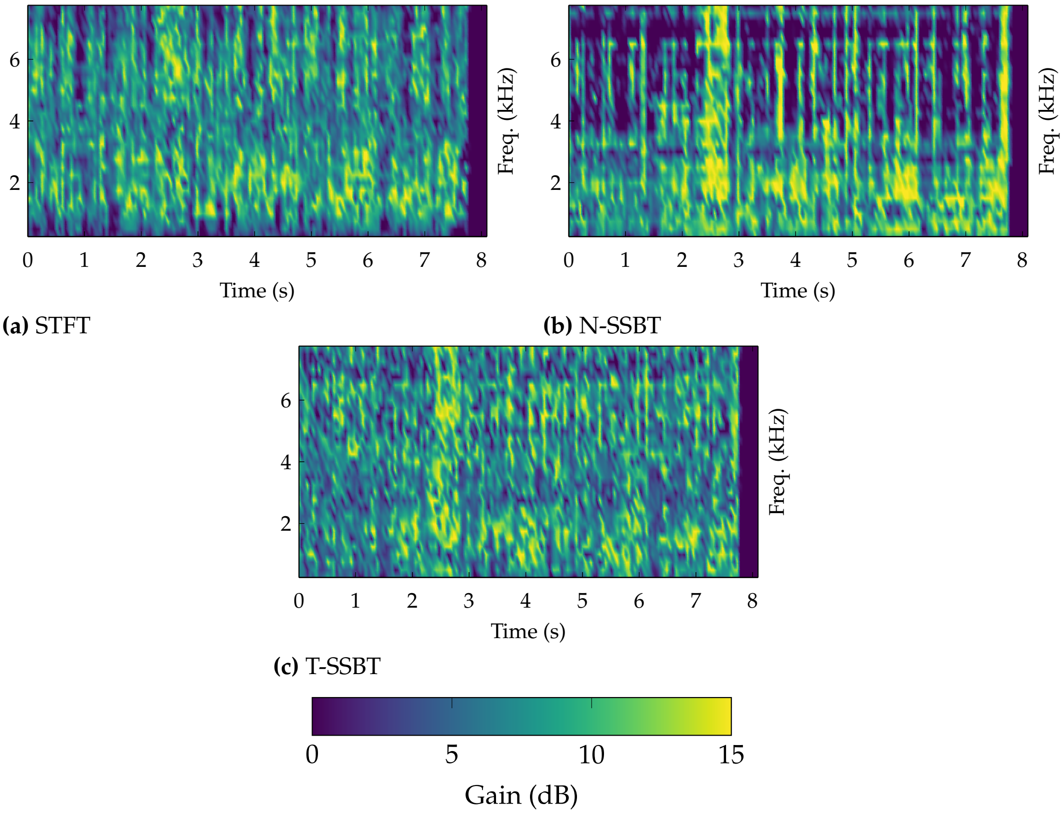

(a) STFT **(b)** N-SSBT **(c)** T-SSBT

Figure 4. Per-window SNR gain for 64 samples/window.

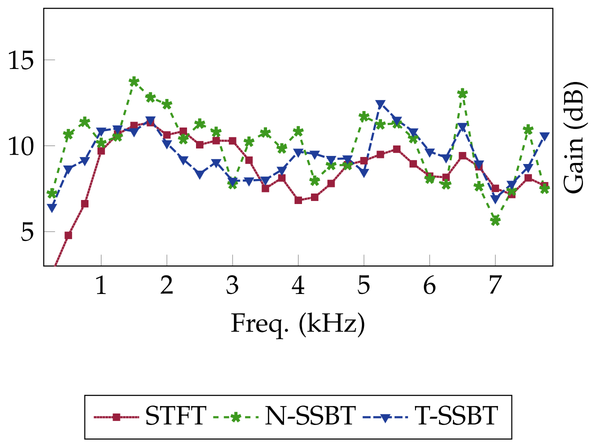

Figure 5. Window-average SNR gain for 64 samples/window.

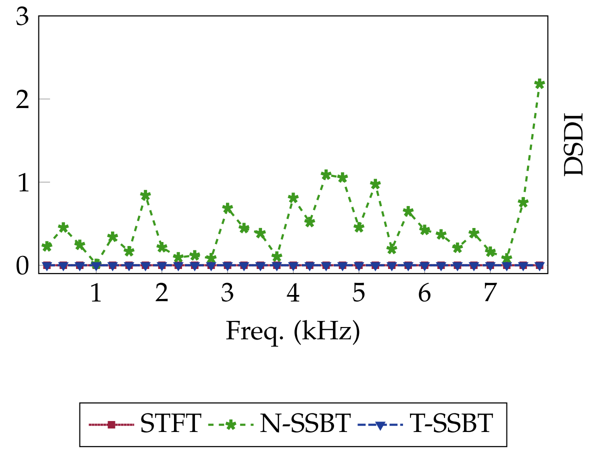

Figure 6. Window-average DSDI for 64 samples/window.

6. Conclusion

In this study, we investigated the application of the Single-Sideband Transform in beamforming within a reverberant environment, utilizing the convolutive transfer function model for filter bank (i.e., the beamformer) estimation. We implemented a Minimum-Variance Distortionless-Response beamformer to enhance signals in a real-life-like scenario, elucidating the process to achieve a true-distortionless MVDR beamformer when employing the SSB transform. The results demonstrated that both the naive MVDR and the true-MVDR beamformers, designed using the SSBT, outperformed the traditional beamformer obtained via the Short-Time Fourier Transform. The naive MVDR exhibited some distortion on the desired signal, whereas the true-MVDR achieved a distortionless response, as expected.

Future research avenues may explore the integration of this transform into different beamformers, or undertake further comparisons against the established and reliable STFT methodology.

Author Contributions: Conceptualization, I. Cohen and V. Curtarelli; Methodology, V. Curtarelli; Software, V. Curtarelli; Writing—original draft: V. Curtarelli; Writing—review and editing, I. Cohen and V. Curtarelli; Supervision, V. Curtarelli. All authors have read and agreed to the published version of the manuscript.

Funding: This research was supported by the Pazy Research Foundation, and the Israel Science Foundation (grant no. 1449/23).

Data Availability Statement: The source-code for the simulations developed here is available at https://github.com/VCurtarelli/py-ssb-ctf-bf.

Conflicts of Interest: The authors declare no conflict of interest.

Abbreviations

The following abbreviations are used in this manuscript:

CTF	Convolutive Transfer Function
DSDI	Desired Signal Distortion Index
LCMV	Linearly-Constrained Minimum-Variance
MVDR	Minimum-Variance Distortionless-Response
SNR	Signal-to-Noise Ratio
SSBT	Single-Sideband Transform
STFT	Short-Time Fourier Transform

Appendix A. SSBT Convolution

Let $x[n]$ be a time domain signal, with $X_{\mathcal{F}}[l,k]$ being its STFT equivalent, and $X_{\mathcal{S}}[l,k]$ its SSBT equivalent. We here assume that both the STFT and the SSBT have K frequency bins. $X_{\mathcal{S}}[l,k]$ can be obtained using $X_{\mathcal{F}}[l,k]$, through

$$X_{\mathcal{S}}[l,k] = -{X_{\mathcal{F}}}^{\Re}[l,k] + {X_{\mathcal{F}}}^{\Im}[l,k] \tag{A1}$$

win which $(\cdot)^{\Re}$ and $(\cdot)^{\Im}$ represent the real and imaginary components of their argument, respectively.

It is easy to see that

$$X_{\mathcal{F}}[l,k] = \frac{1}{\sqrt{2}}\left(e^{-\jmath\frac{3\pi}{4}}X_{\mathcal{S}}[l,k] + e^{\jmath\frac{3\pi}{4}}X_{\mathcal{S}}[l,K-k]\right) \tag{A2}$$

As stated before, this formulation isn't valid for $k=0$ and $k={}^{K}/_{2}$ if K is even, but in these cases $X_{\mathcal{F}}[l,k] = X_{\mathcal{S}}[l,k]$.

Now, let there also be $h[n]$, $H_{\mathcal{F}}[k]$ and $H_{\mathcal{S}}[k]$, with the same assumptions as before. We define $Y_{\mathcal{F}}[l,k]$ and $Y_{\mathcal{S}}[l,k]$ as the output of an LTI system with impulse response $h[n]$, such that

$$Y_{\mathcal{F}}[l,k] = H_{\mathcal{F}}[k]X_{\mathcal{F}}[l,k] \tag{A3a}$$
$$Y_{\mathcal{S}}[l,k] = H_{\mathcal{S}}[k]X_{\mathcal{S}}[l,k] \tag{A3b}$$

We will assume that the MTF model [**?**] correctly models the convolution here. Here we use the MTF model instead of the CTF for simplicity, as these derivations would work exactly the same for the CTF.

Applying Eq. (A1) in Eq. (A3b), and knowing that $X_{\mathcal{F}}[l,k] = X^*_{\mathcal{F}}[l,K-k]$ (same for $H_{\mathcal{F}}[k]$), with $(\cdot)^*$ representing the complex-conjugate; we get that

$$\begin{aligned} Y_{\mathcal{S}}[l,k] &= X_{\mathcal{F}}{}^{\Re}[l,k]H_{\mathcal{F}}{}^{\Re}[l,k] - X_{\mathcal{F}}{}^{\Re}[l,k]H_{\mathcal{F}}{}^{\Im}[l,k] \\ &\quad - X_{\mathcal{F}}{}^{\Im}[l,k]H_{\mathcal{F}}{}^{\Re}[l,k] + X_{\mathcal{F}}{}^{\Im}[l,k]H_{\mathcal{F}}{}^{\Im}[l,k] \\ Y_{\mathcal{S}}[l,K-k] &= X_{\mathcal{F}}{}^{\Re}[l,k]H_{\mathcal{F}}{}^{\Re}[l,k] + X_{\mathcal{F}}{}^{\Re}[l,k]H_{\mathcal{F}}{}^{\Im}[l,k] \\ &\quad + X_{\mathcal{F}}{}^{\Im}[l,k]H_{\mathcal{F}}{}^{\Re}[l,k] + X_{\mathcal{F}}{}^{\Im}[l,k]H_{\mathcal{F}}{}^{\Im}[l,k] \end{aligned} \tag{A4}$$

Passing this through Eq. (A2),

$$\begin{aligned} Y'_{\mathcal{F}}[l,k] = &- X_{\mathcal{F}}{}^{\Re}[l,k]H_{\mathcal{F}}{}^{\Re}[l,k] + \mathrm{j}X_{\mathcal{F}}{}^{\Re}[l,k]H_{\mathcal{F}}{}^{\Re}[l,k] \\ &+ \mathrm{j}X_{\mathcal{F}}{}^{\Im}[l,k]H_{\mathcal{F}}{}^{\Re}[l,k] - X_{\mathcal{F}}{}^{\Im}[l,k]H_{\mathcal{F}}{}^{\Im}[l,k] \end{aligned} \tag{A5}$$

where $Y'_{\mathcal{F}}[l,k]$ is the STFT-equivalent of $Y_{\mathcal{S}}[l,k]$.

Expanding Eq. (A3a) in terms of real and imaginary components,

$$\begin{aligned} Y_{\mathcal{F}}[l,k] = &\, X_{\mathcal{F}}{}^{\Re}[l,k]H_{\mathcal{F}}{}^{\Re}[l,k] + \mathrm{j}X_{\mathcal{F}}{}^{\Re}[l,k]H_{\mathcal{F}}{}^{\Im}[l,k] \\ &+ \mathrm{j}X_{\mathcal{F}}{}^{\Im}[l,k]H_{\mathcal{F}}{}^{\Re}[l,k] - X_{\mathcal{F}}{}^{\Im}[l,k]H_{\mathcal{F}}{}^{\Im}[l,k] \end{aligned} \tag{A6}$$

Comparing Eq. (A5) and Eq. (A6), it is trivial to see that $Y'_{\mathcal{F}}[l,k] \neq Y_{\mathcal{F}}[l,k]$. This proves that the SSBT doesn't appropriately models the convolution, and therefore the convolution theorem doesn't hold when applying this transform.

References

1. Lobato, W.; Costa, M.H. Worst-Case-Optimization Robust-MVDR Beamformer for Stereo Noise Reduction in Hearing Aids. *IEEE/ACM Transactions on Audio, Speech, and Language Processing* **2020**, *28*, 2224–2237. https://doi.org/10.1109/TASLP.2020.3009831.
2. Chen, J.; Kung Yao.; Hudson, R. Source localization and beamforming. *IEEE Signal Processing Magazine* **2002**, *19*, 30–39. https://doi.org/10.1109/79.985676.
3. Lu, Y. BIOMEDICAL ULTRASOUND BEAM FORMING. *Ultrasound in Med. & Biol.* **1994**, *20*, 403–428. https://doi.org/10.1016/0301-5629(94)90097-3.
4. Nguyen, N.Q.; Prager, R.W. Minimum Variance Approaches to Ultrasound Pixel-Based Beamforming. *IEEE Transactions on Medical Imaging* **2017**, *36*, 374–384. https://doi.org/10.1109/TMI.2016.2609889.
5. Benesty, J.; Cohen, I.; Chen, J. *Fundamentals of signal enhancement and array signal processing*; John Wiley & Sons Singapore Pte. Ltd: Hoboken, 2018.
6. Kıymık, M.; Güler, İ.; Dizibüyük, A.; Akın, M. Comparison of STFT and wavelet transform methods in determining epileptic seizure activity in EEG signals for real-time application. *Computers in Biology and Medicine* **2005**, *35*, 603–616. https://doi.org/10.1016/j.compbiomed.2004.05.001.
7. Pan, C.; Chen, J.; Shi, G.; Benesty, J. On microphone array beamforming and insights into the underlying signal models in the short-time-Fourier-transform domain. *The Journal of the Acoustical Society of America* **2021**, *149*, 660–672. https://doi.org/10.1121/10.0003335.
8. Chen, W.; Huang, X. Wavelet-Based Beamforming for High-Speed Rotating Acoustic Source. *IEEE Access* **2018**, *6*, 10231–10239. https://doi.org/10.1109/ACCESS.2018.2795538.
9. Yang, Y.; Peng, Z.K.; Dong, X.J.; Zhang, W.M.; Meng, G. General Parameterized Time-Frequency Transform. *IEEE Transactions on Signal Processing* **2014**, *62*, 2751–2764. https://doi.org/10.1109/TSP.2014.2314061.
10. Almeida, L. The fractional Fourier transform and time-frequency representations. *IEEE Transactions on Signal Processing* **1994**, *42*, 3084–3091. https://doi.org/10.1109/78.330368.

11. Crochiere, R.E.; Rabiner, L.R. *Multirate digital signal processing*; Prentice-Hall signal processing series, Prentice-Hall: Englewood Cliffs, NJ, 1983.
12. Oyzerman, A. Speech Dereverberation in the Time-Frequency Domain. Master's thesis, Technion - Israel Institute of Technology, Haifa, Israel, 2012.
13. Talmon, R.; Cohen, I.; Gannot, S. Relative Transfer Function Identification Using Convolutive Transfer Function Approximation. *IEEE Transactions on Audio, Speech, and Language Processing* **2009**, *17*, 546–555. https://doi.org/10.1109/TASL.2008.2009576.
14. Kumatani, K.; McDonough, J.; Schacht, S.; Klakow, D.; Garner, P.N.; Li, W. Filter bank design based on minimization of individual aliasing terms for minimum mutual information subband adaptive beamforming. In Proceedings of the 2008 IEEE International Conference on Acoustics, Speech and Signal Processing, Las Vegas, NV, March 2008; pp. 1609–1612. https://doi.org/10.1109/ICASSP.2008.4517933.
15. Gopinath, R.; Burrus, C. A tutorial overview of filter banks, wavelets and interrelations. In Proceedings of the 1993 IEEE International Symposium on Circuits and Systems, Chicago, IL, USA, 1993; pp. 104–107. https://doi.org/10.1109/ISCAS.1993.393668.
16. Capon, J. High-resolution frequency-wavenumber spectrum analysis. *Proceedings of the IEEE* **1969**, *57*, 1408–1418. https://doi.org/10.1109/PROC.1969.7278.
17. Erdogan, H.; Hershey, J.R.; Watanabe, S.; Mandel, M.I.; Roux, J.L. Improved MVDR Beamforming Using Single-Channel Mask Prediction Networks. In Proceedings of the Interspeech 2016. ISCA, September 2016, pp. 1981–1985. https://doi.org/10.21437/Interspeech.2016-552.
18. DeMuth, G. Frequency domain beamforming techniques. In Proceedings of the ICASSP '77. IEEE International Conference on Acoustics, Speech, and Signal Processing, Hartford, CT, USA, 1977; Vol. 2, pp. 713–715. https://doi.org/10.1109/ICASSP.1977.1170316.
19. Habets, E.A.P.; Benesty, J.; Gannot, S.; Naylor, P.A.; Cohen, I. On the application of the LCMV beamformer to speech enhancement. In Proceedings of the 2009 IEEE Workshop on Applications of Signal Processing to Audio and Acoustics, New Paltz, NY, October 2009; pp. 141–144. https://doi.org/10.1109/ASPAA.2009.5346463.
20. Habets, E. RIR Generator, 2020.
21. Nielsen, J.K.; Jensen, J.R.; Jensen, S.H.; Christensen, M.G. The Single- and Multichannel Audio Recordings Database (SMARD). In Proceedings of the Int. Workshop Acoustic Signal Enhancement, Sep. 2014.
22. Johnson, D.H. Signal Processing Information Database, 2013.